crystals

MDPI

Article

Preparation, Crystal Structure and Luminescence Properties of Lanthanide Complexes with 2,4,6-tri(pyridin-2-yl)-1,3,5-triazine and Organic Carboxylic Acid

Jingjing Li [1,2], Xueqiong Zhang [1], Bin Yue [1], Ailing Wang [1], Lingjuan Kong [1], Jian Zhou [1], Haibin Chu [1,*] and Yongliang Zhao [1,*]

[1] College of Chemistry and Chemical Engineering, Inner Mongolia University, Huhhot 010021, China; hxlijingjing@163.com (J.L.); xmlqzxq1990@163.com (X.Z.); yuebin@boe.com.cn (B.Y.); godlovewal@163.com (A.W.); klj19910825@163.com (L.K.); hxzhoujian@163.com (J.Z.)

[2] Hulun Buir Institute of Environmental Science, Hulun Buir 021008, China

* Correspondence: chuhb@imu.edu.cn (H.C.); hxzhaoyl@163.com (Y.Z.); Tel. +86-0471-499-2692; Fax: +86-471-499-2981

Academic Editor: Ingo Hartenbach
Received: 1 April 2017; Accepted: 10 May 2017; Published: 14 May 2017

Abstract: Five crystal complexes $\{[Eu_2(TPTZ)_2(mNBA)_6(H_2O)_2]\cdot 2CH_3OH\}_n$ (1), $[Eu(TPTZ)(CF_3COO)(H_2O)_5]\cdot Cl_2\cdot CH_3CH_2OH$ (2), $\{[Yb_2(TPTZ)_2(BDC)_3]\cdot 2H_2O\}_n$ (3), $[Yb(TPTZ)Cl(H_2O)_4]\cdot Cl_2$ (4) and $[Er(TPTZ)(TTA)Cl_2]$ (5) (*m*NBA = *m*-nitro benzoate, BDC = terephthalate, TTA = thenoyltrifluoroacetone, TPTZ = 2,4,6-tri(2-pyridyl)-1,3,5-triazine) have been synthesized. The single X-ray diffraction reveals that TPTZ is mainly in the trident coordination mode and organic aromatic carboxylic acids are in the multiple coordination modes in the crystals. The composition of solvents, reaction temperature and reactant ratios all affect the composition and structure of the formed crystals. Crystals 1 and 3 belong to triclinic system, while the other three belong to monoclinic system. Among them, Crystal complexes 1 and 3 are coordination polymers. The other three crystals are mononuclear complexes with Ln^{III} ions in the asymmetric environment. Both of the Crystal complexes 1 and 2 show strong luminescence emissions of Eu^{3+}. The luminescence lifetimes of the two complexes are 0.761 ms and 0.447 ms, respectively. In addition, their luminescence quantum efficiencies are 25.0% and 16.7%, respectively.

Keywords: lanthanide complexes; 2,4,6-tri(pyridin-2-yl)-1,3,5-triazine; aromatic carboxylic acids; crystal structure; luminescence

1. Introduction

The lanthanide complexes have a great deal of applications in the fields such as single-molecule magnets, biomedicine, electro-luminescence devices, laser-systems and optical communications [1–5]. However, f-f electron transitions of lanthanide ions are forbidden by the parity rule. Thus, their fluorescent intensities and quantum efficiencies are relatively low [6]. Some neutral or anionic organic ligands, such as aromatic carboxylic acid, have been introduced. These organic ligands have excellent light absorption abilities and can transfer energy to lanthanide ions due to so-called "antenna effect" [7,8]. Because of the distinctive coordination modes and conjugated large π system, neutral ligand 2,4,6-tri(pyridin-2-yl)-1,3,5-triazine (TPTZ) has become one of the most attractive ligands. Moreover, TPTZ can increase the chemical and thermal stability of the complexes [9–14]. In addition, the triplet energy level of TPTZ (21,200 cm^{-1}) matches the lowest excited state energy level of Eu^{3+} (17,200 cm^{-1}), which results in the enhancement of the luminescence intensities of europium

complexes [15,16]. Up to now, crystals of Sm, Eu, Tb, Dy, Gd, Nd, Cd, Cu and Co with TPTZ have been synthesized [17–20].

The anionic ligand terephthalic acid (H_2BDC) may bind with metal ions by bidentate chelating coordination or monodentate bridging coordination, which can form one-dimensional chains, two-dimensional layered structures and three-dimensional network structures with distinct topologies [21–26]. *m*-nitrobenzoic acid (*m*NBA) and thenoyltrifluoroacetone (TTA) ligands are also typical organic ligands, which can form stable complexes with lanthanide ions [27–29]. In recent years, constructing crystals and coordination polymers have become a hot spot in the material and coordination chemistry research. Because lanthanide ions possess high and variable coordination number, and complicated structure, the synthesis of the lanthanide crystal complexes and the coordination polymers are typically unpredictable [30–34]. Herein, we introduce the neutral ligand of TPTZ together with the different anionic ligands H_2BDC, *m*NBA and TTA, using the methods of solvothermal and slow evaporation of solvent by varying the reaction conditions. Five crystal complexes with distinct composition and structure have been synthesized with central ions of Eu, Yb and Er. In addition, the luminescence properties of the europium complexes have been discussed.

2. Experimental Section

2.1. Chemical Reagents and Instruments

The purity of lanthanide oxides Eu_2O_3, Yb_2O_3 and Er_2O_3 are all 99.99%. TPTZ, H_2BDC, *m*NBA, TTA and other reagents are all of analytical grade and used as received. Elemental analysis of C, H and N was performed on a Vario EL Cube elemental analyzer (Hanau, Germany). Crystal X-ray diffraction patterns were recorded on a Bruker SMART 1000 CCD diffractometer (Bruker, karlsruhe, Germany) with a monochromator in the Mo and Cu Kα radiation (λ = 0.71073/1.54184 Å) incident beam at a temperature of 293 K. Infrared spectra were recorded with KBr pellets on a Nicolet Nexus 670 FT-IR spectrometer (Madison, WI, USA) within the scope of 4000–400 cm^{-1}. Luminescence spectra and luminescence lifetime of the europium complexes were measured on an Edinburgh Analytical Instruments FLS-920 spectraphotometer (Edinburgh, UK). Quantum efficiencies were calculated according to literature and illustrated in support information.

2.2. Synthesis of Crystal Complexes 1–5

For the experiment, 1.76 g Eu_2O_3 was dissolved in hydrochloric acid under constant stirring. The mixture was heated until the crystallized film appeared, after which the solution was cooled to room temperature and a white powder appeared. The white powder was collected and dissolved in anhydrous ethanol solution to get a 0.1 mol L^{-1} $EuCl_3$ ethanol solution. The preparation procedures of $YbCl_3$ and $ErCl_3$ ethanol solutions were similar to that of the $EuCl_3$ solution.

{[Eu_2(TPTZ)$_2$(mNBA)$_6$(H_2O)$_2$]·2CH_3OH}$_n$ (1). A mixture of *m*NBA (3 mmol, 0.501 g) and $EuCl_3$ (1 mmol) were dissolved in 15 mL anhydrous ethanol solution, stirred and heated to 50 °C for 3 h. The pH value of the solution was adjusted to 6.2–6.7 with dilute ammonia solution until white precipitate appeared. The solution was left still at room temperature overnight. Then, the mixture was separated by filtering. After being washed with pure ethanol, the white precipitate of Eu(*m*NBA)$_3$ complex was dried to constant weight. The precipitate was dissolved in 30 mL of CH_2Cl_2 and five drops of DMF. Then, a methanol solution of TPTZ (1 mmol, 0.312 g) was added dropwise into the solution. The solution was sealed with plastic wrap and evaporated automatically for seven days. Faint yellow crystal complex was finally collected—Anal. Calc. (%) for crystal complex [$C_{80}H_{60}Eu_2N_{18}O_{28}$]$_n$: C, 47.40; H, 2.96; N, 12.44; found: C, 46.94; H, 2.70; N, 12.23.

[Eu(TPTZ)(CF_3COO)(H_2O)$_5$]·Cl_2 CH_3CH_2OH (2). A mixture of TTA (1 mmol, 0.222 g) and $EuCl_3$ (1 mmol) was dissolved in a mixture solvent of 10 mL ethanol and 5 mL acetonitrile. The pH value of the solution was adjusted to 6.4 with dilute ammonia solution and white precipitate was obtained. After stirring at room temperature for 30 min, TPTZ (1 mmol, 0.312 g) was added. The solution was kept stirring for 30 min and transferred into a Teflon-lined stainless steel autoclave. The autoclave was kept for 72 h under 120 °C and programmed cooled to room temperature, after which the

crystal complex was obtained—Anal. Calc. (%) for crystal complex $C_{22}H_{28}Cl_2EuF_3N_6O_8$: C, 33.66; H, 3.56; N, 10.71; found: C, 33.54; H, 3.20; N, 11.03.

{[Yb_2(TPTZ)$_2$(BDC)$_3$]·2H_2O}$_n$ (3). H_2BDC (1 mmol, 0.166 g) was dissolved in a mixture solvent of 7 mL DMF and 5 mL distilled water. Then, 1 mmol of $YbCl_3$ ethanol solution was added into the stock solution. After stirring for about 30 min, TPTZ (1 mmol, 0.312 g) was added to the solution. The solution was stirred at room temperature for another 30 min. Then, the solution was transferred into a Teflon-lined stainless steel autoclave and reacted at 100 °C for 72 h. After being programmed and cooled to room temperature, the crystal complex was obtained—Anal. Calc. (%) for crystal complex $[C_{60}H_{40}N_{12}O_{14}Yb_2]_n$: C, 48.03; H, 2.67; N, 11.20; found: C, 48.07; H, 2.69; N, 11.31.

[Yb(TPTZ)Cl(H_2O)$_4$]·Cl_2 (4). TPTZ (0.5 mmol, 0.156 g) was dissolved in 10 mL acetonitrile. $YbCl_3$ (1.5 mmol) ethanol solution was slowly added into the solution. The pH value of the solution was then adjusted to 6.4 with ammonia solution. After stirring at room temperature for 30 min, the solution was transferred to a Teflon-lined stainless steel autoclave and reacted for 72 h under 120 °C. After programmed cooled to room temperature, the crystal complex was obtained—Anal. Calc. (%) for crystal complex $C_{18}H_{20}Cl_3N_6O_4Yb$: C, 32.47; H, 3.01; N, 12.65; found: C, 32.03; H, 2.87; N, 12.16.

[Er(TPTZ)(TTA)Cl$_2$] (5). TTA (1 mmol, 0.222 g) was dissolved in a mixture solvent of 10 mL ethanol and 5 mL acetonitrile. Then $ErCl_3$ (1 mmol) ethanol solution was added. After stirring at room temperature for 30 min, TPTZ (1 mmol, 0.312 g) was added. The solution was kept stirring for 30 min and transferred into a Teflon-lined stainless steel autoclave to react for 72 h under 80 °C. After being programmed and cooled to room temperature, the crystal complex was obtained—Anal. Calc. (%) for crystal complex $C_{26}N_6O_2SF_3H_{16}Cl_2Er$: C, 40.47; H, 2.09; N, 10.89; found: C, 40.94; H, 2.40; N, 10.53.

2.3. Crystal Structure Determinations

The crystal data have been collected by a Xcalibur Eos Gemini diffractometer (South San Francisco, CA, US) using Mo and Cu Kα radiation incident beam. All structures were solved by direct methods and refined by full-matrix least-squares methods against F^2 with SHELXTL-97. Diamond-crystal and molecular visualization software was applied in drawing crystal figures. All of the non-hydrogen atoms were refined with anisotropic thermal parameters, and all hydrogen atoms have been omitted for the sake of clarity. Crystallographic data of the crystals have been deposited at the Cambridge Crystallographic Data Center (England, Britain). The CCDC numbers of the five Crystals 1–5 are 960822, 960824, 960826, 960821 and 960823, respectively.

3. Results and Discussion

3.1. Infrared Spectroscopy

The IR spectra of the five crystal complexes and the ligands were shown in Figure 1. For TPTZ ligand, the band at 1370 cm^{-1} was attributed to the breathing vibration of the center ring and the band at 993 cm^{-1} was attributed to the bending vibration of the pyridyl ring. The two bands shifted to 1383–1382 and 1012–1008 cm^{-1} in the Crystal complexes 1–5, respectively, indicating that nitrogen atoms of the center ring and the pyridyl ring were coordinated with the metal ions [15,16]. The bands observed in the 767–771 cm^{-1} region were assigned to the aromatic C-H deformation vibrations [15,35]. In addition, the complexes 1-4 exhibited a band in the 1645–1623 cm^{-1} region, which could be assigned to $\delta_{(OH)}$ of H_2O [35]. The absorption band of ligand H_2BDC showed a typical band around 1681 cm^{-1}, which may be ascribed to the stretching vibration of carbonyl $\upsilon_{(C=O)}$. This band disappeared in the complexes. After coordinated with Yb^{3+} ions in complex 3, the asymmetric stretching vibrations of the COO^- groups located at 1636 and 1551 cm^{-1}, while the symmetric stretching vibrations absorption appeared at 1530 and 1425 cm^{-1}. The $\Delta\upsilon_{as-s}$ [$\Delta\upsilon_{as-s} = \upsilon_{as}(COO) - \upsilon_s(COO)$] value is used to determine the coordination mode between the metal and the carboxylate ligand. It is generally believed that $\Delta\upsilon_{as-s}$ is below 200 cm^{-1} for the bidentate and bridging mode, but greater than 200 cm^{-1} for the unidentate mode [36–39]. The $\Delta\upsilon_{as-s}$ values are between 106 and 126 cm^{-1}, respectively, and suggest that the COO^- groups are coordinated in the bidentate chelate mode

and bridging mode. For TTA, the broad peak around 1654 cm^{-1} ($\upsilon_{as(C=O)}$) of carbonyl shifted to 1593 cm^{-1} in complex 5. Two peaks (1149 cm^{-1} and 1197 cm^{-1}) were assigned to the characteristic peaks of TTA, which shifted to 1143 cm^{-1} and 1193 cm^{-1}. Similarly, 1311 cm^{-1} ($\upsilon_{s(CF3)}$) in TTA shifted to 1306 cm^{-1} in complex 5, which indicated that lanthanide ions coordinated with TTA [27,28,40–43]. For *m*-nitrobenzoic acid (*m*NBA), the characteristic absorption peak around 1693 cm^{-1} may be ascribed to the stretching vibration of carbonyl. In complex 1, the asymmetric stretching vibrations of the COO^- groups exhibited strong absorption bands around 1623 and 1545 cm^{-1}, while the symmetric stretching vibrations absorption bands appeared around 1403 and 1382 cm^{-1}. The $\Delta\upsilon_{as-s}$ values suggest that the COO^- groups are coordinated with Eu^{3+} ions in bidentate chelate, unidentate and bridging mode [29,44].

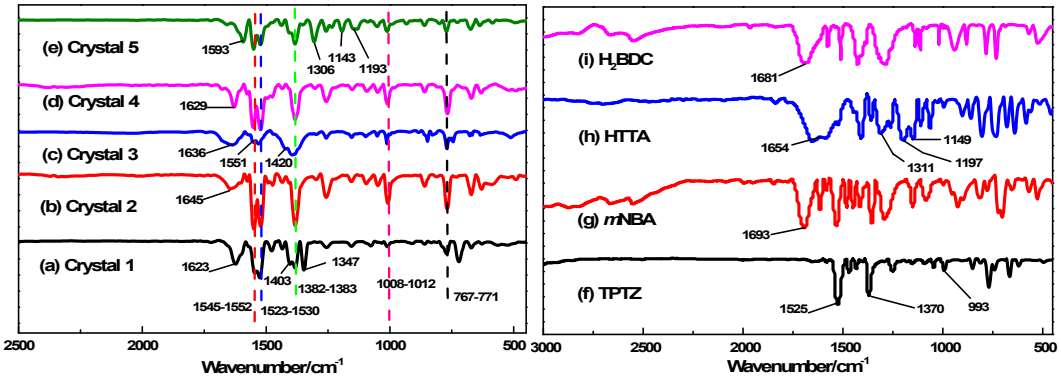

Figure 1. Infrared spectra of five crystal complexes and ligands: (**a**) *{[Eu2(TPTZ)2(mNBA)6(H2O)2]·2CH3OH}n*; (**b**) [Eu(TPTZ)(CF_3COO)(H_2O)$_5$]·Cl_2·CH_3CH_2OH; (**c**) {[Yb_2(TPTZ)$_2$(BDC)$_3$]·2H_2O}$_n$; (**d**) [Yb(TPTZ)Cl(H_2O)$_4$]·Cl_2; (**e**) [Er(TPTZ)(TTA)Cl_2]; (**f**) TPTZ; (**g**) *m*NBA; (**h**) HTTA; (**i**) H_2BDC.

3.2. Structural Analysis and Discussion

The structures of the five crystal complexes were established by single crystal X-ray diffraction at 293(2) K. A summary of the key crystallographic information for the five crystals was listed in Table 1, the main data of selected bond lengths and angles were summarized in Table 2, and more data of bond lengths and bond angles for the five crystals were displayed in supporting information.

Table 1. Crystal data and structure refinement information.

Crystal	**1**	**2**	**3**	**4**	**5**
Formula	$C_{80}H_{60}Eu_2N_{18}O_{28}$	$C_{22}H_{28}Cl_2EuF_3N_6O_8$	$C_{60}H_{40}N_{12}O_{14}Yb_2$	$C_{18}H_{20}Cl_3N_6O_4Yb$	$C_{26}H_{16}Cl_2ErF_3N_6O_2S$
Mr	2025.40	784.36	1499.13	663.79	771.68
T, K	293(2) K	293(2) K	293(2) K	293(2) K	293(2) K
λ (Mo/Cu Kα), Å	0.71073	0.71073	1.54184	0.71073	0.71073
Crystal system	Triclinic	Monoclinic	Triclinic	Monoclinic	Monoclinic
Space group	P-1	C2/c	P-1	P21/c	P21/n
a, Å	10.8765(10)	25.670(2)	9.8997(7)	11.9058(12)	10.0669(11)
b, Å	11.733(8)	16.3284(6)	9.9032(5)	24.7081(19)	20.4848(16)
c, Å	16.7469(17)	16.8617(12)	17.7324(11)	7.8908(8)	13.3962(10)
α, deg	76.330(7)	90	81.704(5)	90	90
β, deg	82.130(8)	121.440(5)	74.458(6)	93.380(10)	93.717(8)
γ, deg	83.204(6)	90	69.889(5)	90	90
V, Å^3	2048.8(3)	6030.0(7)	1570.17(16)	2317.2(4)	2756.7(4)
Z	2	8	2	4	4
Dc, g cm^{-3}	1.642	1.728	1.585	1.956	1.859
μ, mm^{-1}	0.866	2.330	3.032	1.161	3.371
θ range, (°)	2.41–28.75	2.69–25.02	2.44–25.02	2.71–28.77	2.51–25.02
Index range	−14/9, −14/15, −22/22	−30/30, −19/18, −19/20	−11/11, −11/11, −18/21	−13/14, −29/26, −9/8	−11/11, −24/22, −15/14
Reflections unique; collected	9181 [R_{int} = 0.0592]	5316 [R_{int} = 0.1245]	5407 [R_{int} = 0.1046]	5259 [R_{int} = 0.0639]	4798 [R_{int} = 0.1077]

	16,229	18,834	10,434	10,505	12,982
GOF	1.046	1.046	1.027	1.037	0.973
Final Rindices	R_1 = 0.0489,	R_1 = 0.0907,	R_1 = 0.0639,	R_1 = 0.0487,	R_1 = 0.0598,
[I > 2σ]	wR_2 = 0.0697	wR_2 = 0.2099	wR_2 = 0.1426	wR_2 = 0.0693	wR_2 = 0.0906
Rindices	R_1 = 0.0710,	R1 = 0.1581, wR_2 =	R_1 = 0.0978,	R_1 = 0.0824,	R_1 = 0.1226,
(all data)	wR_2 = 0.0810	0.2584	wR_2 = 0.1992	wR_2 = 0.0852	wR_2 = 0.1199

{[Eu$_2$(TPTZ)$_2$(mNBA)$_6$(H$_2$O)$_2$]·2CH$_3$OH}$_n$ (1). Crystal 1 belongs to coordination polymer and crystallizes in a triclinic system, P-1 space group. Each asymmetric unit consists of one Eu ^{III} ion, one TPTZ, three *m*NBA and one coordinated water molecule (Figure 2). The distance between the two Eu ^{III} ions is 5.088 Å. The two Eu ^{III} ions have the same coordination environment and the two Eu ^{III} ions were bridged by two *m*-nitrobenzoic acid. In addition, TPTZ adopts tridentate coordination with europium ions and forms a 1:1 europium/TPTZ compound [45]. The coordination number of europium ion is 9. Each Eu ^{III} ion coordinately bonds to three nitrogen atoms of one TPTZ (N_1, N_2, N_5), five oxygen atoms from four *m*NBA ions (O_1, O_2, O_5, O_6, O_9) and one oxygen atom from the coordinated water molecule (O_{13}). From Table 2, the bond angles of three N-M-N are 62.69° for N_2-Eu_1-N_5, 124.46° for N_1-Eu_1-N_5 and 61.80° for N_2-Eu-N_1, respectively. The *m*NBA takes a variety of coordination modes with Eu ^{III} ion, including monodentate form, bidentate chelating and bridging form. It can be concluded from the data that the Ln ^{III}-O bond length of bidentate chelating is the longest compared with monodentate and bridging coordination.

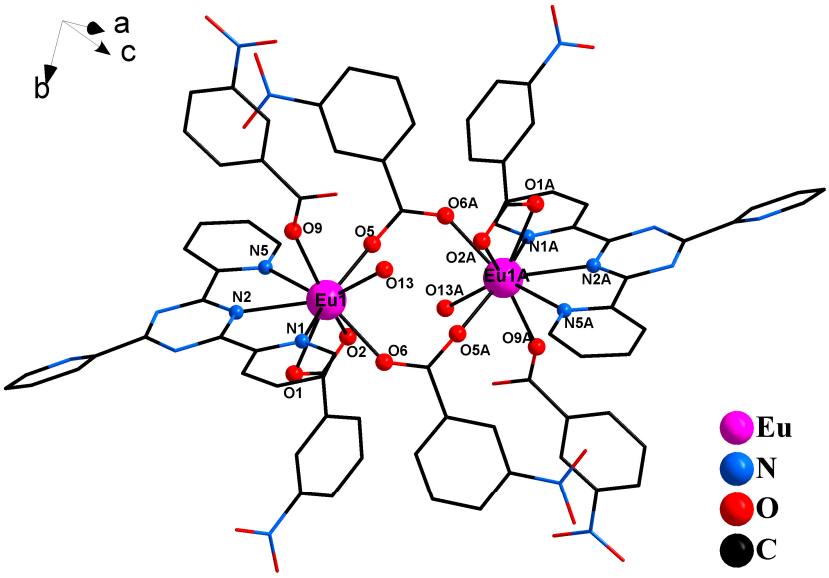

Figure 2. The crystal structure of {[Eu$_2$(TPTZ)$_2$(*m*NBA)$_6$(H$_2$O)$_2$]·2CH$_3$OH}$_n$.

[Eu(TPTZ)(CF$_3$COO)(H$_2$O)$_5$]·Cl$_2$·CH$_3$CH$_2$OH (2). Crystal 2 is a europium compound and crystallizes in a monoclinic system, C2/c space group. Each asymmetric unit consists of one europium ion, one TPTZ ligand, one trifluoroacetate and five coordinated water molecules (Figure 3). Crystal 2 is a mononuclear. The coordination number of Eu ^{III} ion is 9. Eu ^{III} ion coordinately bonds to three nitrogen atoms from one TPTZ (N_1, N_2, N_5), one oxygen atom from trifluoroacetate (O_1) and five oxygen atoms from the coordinated water molecules (O_3,O_4, O_5, O_6, O_7).

{[Yb$_2$(TPTZ)$_2$(BDC)$_3$]·2H$_2$O}$_n$ (3). Crystal 3 is a ytterbium compound and crystallizes in a triclinic system, P-1 space group. The coordination number of Yb ^{III} ion is 9. Yb ^{III} ion coordinately bonds to three nitrogen atoms of one TPTZ (N_1, N_2, N_5) and six oxygen atoms of three BDC^{2-} (O_1, O_2, O_3, O_4, O_5, O_6) (Figure 4). Furthermore, each carboxylate group of the BDC^{2-} takes two coordinate forms linking metal ions. One is bidentate chelating with the coordination mode ($\kappa^2 - \mu_1$). The other is monodentate bridging coordination mode [($\kappa^1 - \kappa^1$) $- \mu_2$]. The Yb-O bond length of bidentate chelating is longer than a monodentate bridging mode, which is the same as Crystal 1. There is no

coordinated water molecule. Four bidentate chelating BDC^{2-} molecules are almost on the same plane.

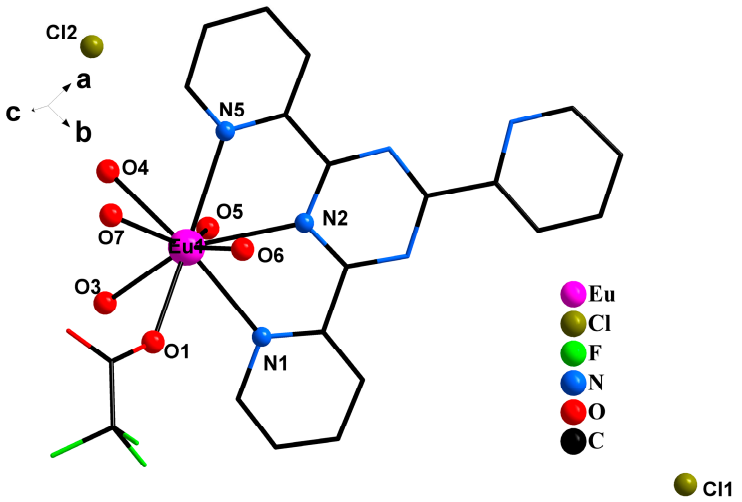

Figure 3. The crystal structure of $[Eu(TPTZ)(CF_3COO)(H_2O)_5]\cdot Cl_2\cdot CH_3CH_2OH$.

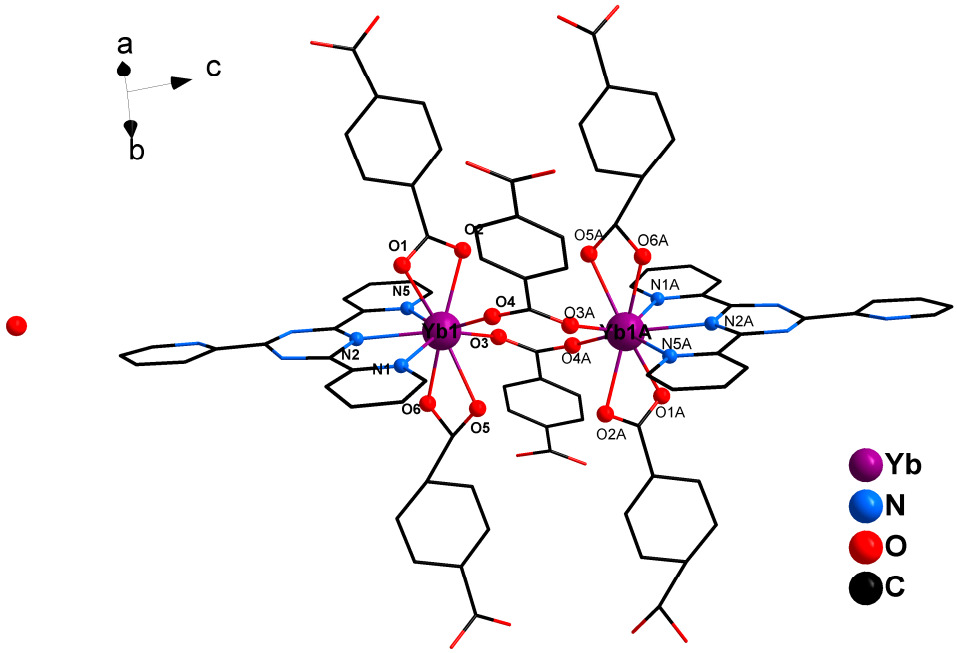

Figure 4. The crystal structure of $\{[Yb_2(TPTZ)_2(BDC)_3]\cdot 2H_2O\}_n$.

$[Yb(TPTZ)Cl(H_2O)_4]\cdot Cl_2$ (4). Crystal 4 is a ytterbium complex and crystallizes in a monoclinic system, P21/c space group. The asymmetric unit of this compound consists of one Yb ^{III} ion, one TPTZ ligand, four coordinated water molecules and one chloride ion (Figure 5). The coordination number of Yb ^{III} ion is 8. In addition, a Yb ^{III} ion coordinately bonds to three nitrogen atoms of one TPTZ (N_1, N_2, N_5), four oxygen atoms of the coordinated water molecules (O_1, O_2, O_3, O_4) and one chloride ion.

$[Er(TPTZ)(TTA)Cl_2]$ (5). Crystal 5 is an erbium complex and crystallizes in a monoclinic system, P21/n space group. The asymmetric unit of the compound contains one Er ^{III} ion, one TPTZ, one TTA and two chloride ions (Figure 6). The coordination sphere consists of three nitrogen atoms from one TPTZ, two carbonyl oxygen atoms from one TTA, and two chloride ions. The coordination number of erbium ion is 7, which is relatively lower than the other four crystals. This is ascribed to the deficiency of ligand and no coordination water.

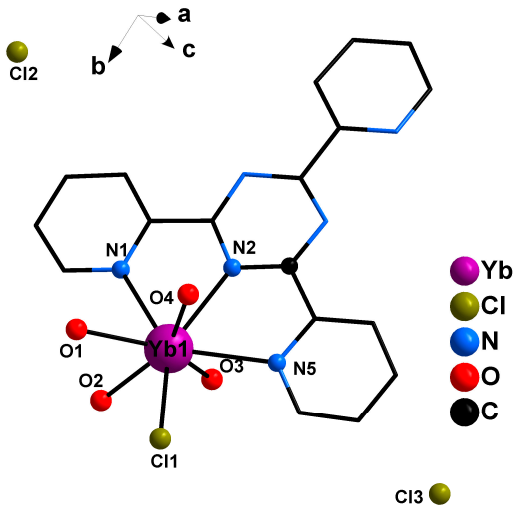

Figure 5. The crystal structure of [Yb(TPTZ)Cl(H_2O)$_4$]·Cl_2.

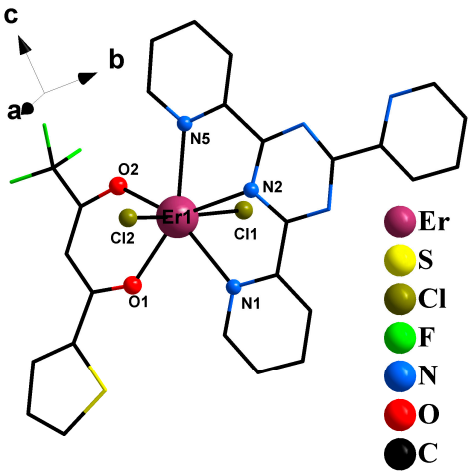

Figure 6. The crystal structure of [Er(TPTZ)(TTA)Cl_2].

As presented in Table 2, Ln-Ln distances in Crystals 1 and 3 are shorter than the other three crystals, which suggest that the Ln-Ln distances in a bi-nuclear structure are shorter than those in a single-nuclear structure. The 2D network structure of Crystal 3 is visualized in Figure 7. As shown in Figure 8, the Eu-Eu distance is shorter than Yb-Yb distance, and the bond angles of O-Eu-O is larger than those of O-Yb-O, which may be related to the larger radius of an Eu ion (94.7 pm) than a Yb ion (86.8 pm) [46] as well as the different coordination modes of Ln ^{III}. Although the coordination number of the two Complexes 1 and 3 are all 9, in the europium complex, Eu ion coordinates with three carboxyls by one bidentate chelating, one monodentate and one bridging coordination. The steric hindrance of this coordination model is smaller than that in the ytterbium complex, in which a Yb ion coordinates with the carboxyl by two bidentate chelating and one bridging coordination. From Table 2, the bond lengths of M-O vary in different crystals. It can be concluded that the difference of bond lengths may be related to the coordination number and steric hindrance of lanthanide complexes. With increasing of the coordination number and the steric hindrance, the bond length of M-O gets longer. The bond lengths of M-O in bidentate chelating are longer when compared with monodentate and bridging coordination.

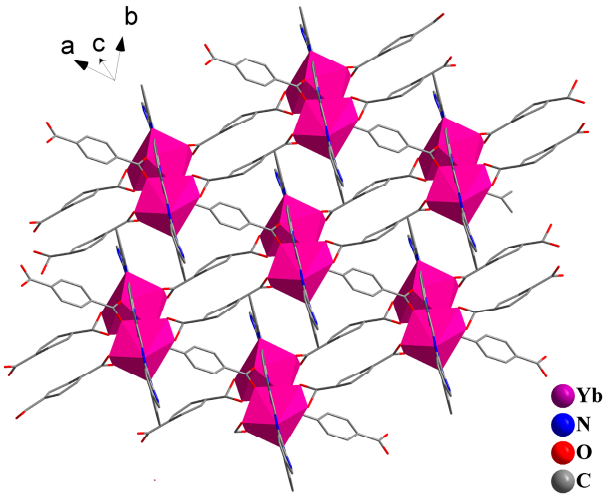

Figure 7. 2D network of crystal 3 $\{[Yb_2(TPTZ)_2(BDC)_3]\cdot 2H_2O\}_n$.

Table 2. Selected bond lengths and bond angles of the five crystals.

Sample	Bond Lengths		Ln—Ln Distance	Bond Angles	
	Ln—O (Å) (Å) [a]	Ln—N		O—Ln—X (°)	N—Ln—N (°) [b]
Crystal 1	Eu_1-O_1 = 2.478(3) Eu_1-O_2 = 2.532(4) Eu_1-O_5 = 2.333(4) Eu_1-O_6 = 2.410(4) Eu_1-O_9 = 2.368(4) Eu_1-O_{13} = 2.503(3)	2.629(5) 2.598(4) 2.635(5)	5.0876(6)	O_1-Eu_1-O_2 = 52.27(11) O_1-Eu_1-O_5 = 124.54(13) O_1-Eu_1-O_9 = 135.39(12) O_5-Eu_1-O_9 = 82.52(13) O_1-Eu_1-O_{13} = 142.85(13) O_6-Eu_1-O_2 = 70.58(14)	61.80(14) 124.46(13) 62.69(14)
Crystal 2	Eu_1-O_1 = 2.420(12) Eu_1-O_3 = 2.446(14) Eu_1-O_4 = 2.497(9) Eu_1-O_5 = 2.406(9) Eu_1-O_6 = 2.435(12) Eu_1-O_7 = 2.437(9)	2.592(10) 2.585(11) 2.628(11)	9.9439(10)	O_1-Eu_1-O_3 = 67.9(5) O_1-Eu_1-O_4 = 120.8(4) O_1-Eu_1-O_5 = 130.5(4) O_1-Eu_1-O_6 = 73.8(5) O_1-Eu_1-O_7 = 73.3(4)	60.7(3) 122.8(3) 62.1(3)
Crystal 3	Yb_1-O_1 = 2.336(13) Yb_1-O_2 = 2.460(13) Yb_1-O_3 = 2.234(13) Yb_1-O_4 = 2.172(11) Yb_1-O_5 = 2.48(3) Yb_1-O_6 = 2.326(15)	2.506(19) 2.482(16) 2.498(19)	5.3109(8)	O_1-Yb_1-O_2 = 53.0(5) O_2-Yb_1-O_4 = 76.4(5) O_3-Yb_1-O_4 = 90.0(4) O_5-Yb_1-O_6 = 43.9(8) O_3-Yb_1-O_5 = 71.2(9) O_1-Yb_1-O_6 = 140.8(5)	63.5(6) 127.9(6) 64.5(5)
Crystal 4	Yb_1-O_1 = 2.385(5) Yb_1-O_2 = 2.336(6) Yb_1-O_3 = 2.289(6) Yb_1-O_4 = 2.325(6) Yb_1-Cl_1 = 2.614(2)	2.524(7) 2.457(7) 2.548(6)	11.9082(11)	O_1-Yb_1-O_2 = 74.7(2) O_2-Yb_1-O_3 = 70.7(2) O_3-Yb_1-O_4 = 141.1(2) O_1-Yb_1-O_3 = 143.2(2) O_1-Yb_1-O_4 = 73.9(2) O_2-Yb_1-O_4 = 148.11(19)	64.1(2) 128.3(2) 64.8(2)
Crystal 5	Er_1-O_1 = 2.280(7) Er_1-O_2 = 2.242(7) Er_1-Cl_1 = 2.577(3) Er_1-Cl_2 = 2.566(3)	2.522(7) 2.434(8) 2.528(7)	8.4679(9)	O_2-Er_1-O_1 = 75.3(2) O_1-Er_1-Cl_2 = 88.65(19) O_2-Er_1-Cl_1 = 90.86(19)	65.2(2) 129.5(3) 64.3(2)

[a] the bond lengths of Ln-N in the order of Ln-N_1, Ln-N_2 to Ln-N_5; [b] the bond angles of N-Ln-N in the order of N_1- Ln -N_2, N_1- Ln -N_5 to N_2- Ln-N_5.

3.3. Effect of Synthetic Methods on the Composition and Structure of Crystal Complexes

The Crystal complex 1 was grown by slow evaporation at room temperature, and the other four crystals were synthesized by the solvothermal method under 80–120 °C. It can be seen that the reactant ratios and synthetic methods have great influences on the composition and structure of these metal-organic complexes, especially on the coordination behavior. Crystal complex 1 was prepared by 1 mmol $EuCl_3$, 1 mmol TPTZ and 3 mmol *m*NBA. Its composition was consistent with the reactant ratio. Crystal complex 2 was prepared by 1 mmol $EuCl_3$, 1 mmol TPTZ and 1 mmol HTTA, but the composition of Crystal complex 2 was $[Eu(TPTZ)(CF_3COO)(H_2O)_5]\cdot Cl_2\cdot CH_3CH_2OH$, which indicated that the ligand TTA decomposed into CF_3COO under120 °C and 72 h. Crystal 3 was prepared by 1 mmol $YbCl_3$, 1 mmol TPTZ and 1 mmol H_2BDC. The composition of Crystal complex 3 was $\{[Yb_2(TPTZ)_2(BDC)_3]\ 2H_2O\}_n$, which indicated that the ligand BDC^{2-} linked Yb^{3+} ions to form polymers in bridging mode. Crystal complex 4 was prepared by 1.5 mmol $YbCl_3$ and 0.5 mmol TPTZ without anionic ligand. The mole ratio of Yb with TPTZ was 3:1, but the composition of Crystal complex 4 was $[Yb(TPTZ)Cl(H_2O)_4]\ Cl_2$, which showed that one TPTZ only combined one Yb ion. Because the organic ligand was lacking in Crystal complex 4, water molecules and chloride ion also participated in coordination. Crystal complex 5 was prepared by $ErCl_3$, TPTZ and TTA with the mole ratio of 1:1:1 at 80 °C. The composition of crystal 5 was $[Er(TPTZ)(TTA)Cl_2]$ with a coordination number of 7. This suggested that TTA did not break down at 80 °C.

In Crystal complex 4, TPTZ coordinates with Yb ions through three nitrogen atoms of the center ring and the pyridyl ring, and the other nitrogen atoms could not coordinate with more Yb ions. However, one TPTZ may coordinate with two monovalent or bivalent transition metal ions [47–49]. This may be because, after coordination between TPTZ and Yb ions, trivalent Yb ions attract more electrons of TPTZ, resulting in lower electron density in other nitrogen atoms. The ligand of organic carboxylate tends to adopt mutiple coordination modes with Ln^{III} and form multinuclear crystals. When the amount of organic ligands is sufficient in the preparation of the complexes, other solvent molecules have difficulty participating in coordination. Crystal complex 1 contains two coordinated water molecules and Crystal complex 3 has no coordinated water molecules. When the organic ligand is lacking, the solvent molecules participate in coordination with Ln^{III} ions. Water molecules generally adopt oxygen atoms coordinated with lanthanide ions. In Crystal complex 2, there are five water molecules and, in Crystal complex 4, there are four water molecules and one chloride ion participating in coordination, respectively. If water molecules are lesser in number, the chlorine ions tend to participate in coordination with Ln^{III} ions, which indicates that the coordination ability of water molecules is greater than chlorine ions. Because of the lack of organic ligands and water molecules, two chloride ions also participate in coordination in Crystal complex 5.

Compared with Crystal complex 5, the TTA was broken down into small molecules (CF_3COO^-) in Crystal complex 2 when the reaction was kept at 120 °C for a long time.

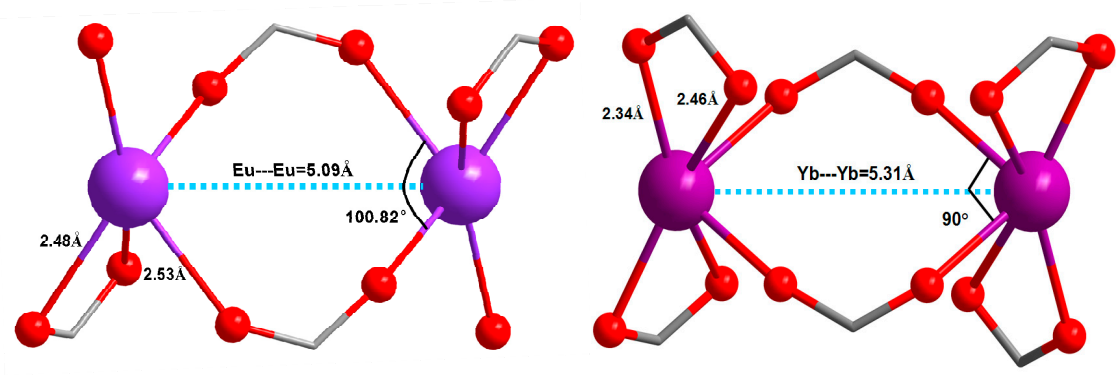

Figure 8. The distance and angles between two metals in Crystal complexes 1 and 3.

3.4. Luminescence of the Europium Complexes

Emission and excitation peaks of Complexes 1 and 2 were measured in solid state under 0.1 nm slit widths at room temperature. The excitation spectra of the europium complexes were measured by monitoring the emission wavelength at 616 nm (Figure S8). The emission spectra were measured at room temperature under the optimal excitation wavelength at 318 nm for Complex 1 and 356 nm for Complex 2 within the scope of 450–750 nm (Figure 9). Both of the emission spectra of Complexes 1 and 2 show five typical emission bands corresponding to the $^5D_0 \rightarrow {}^7F_{0,1,2,3,4}$ transitions of the Eu^{3+}. The two spectra do not show a significant difference, suggesting that the light-emitting sites in Complex 1 are the same as those in Complex 2. Among the five emission bands, the electric dipole transition $^5D_0 \rightarrow {}^7F_2$ around 616 nm is the strongest. In addition, the ratio of electric dipole transition and magnetic dipole transition ($^5D_0 \rightarrow {}^7F_1$) of Complexes 1 and 2 are 3.31 and 4.28, respectively, which indicates that the coordination environment of Eu^{3+} complexes are not center symmetric [50–54]. The luminescence intensities of electric dipole transition of Complexes 1 and 2 are 0.74×10^5 and 1.4×10^5, respectively. The emission intensity of Complex 2 is stronger than that of Complex 1. The energy difference between the triplet energy level of *m*NBA and Eu^{3+} excited state energy is approximately 8000 cm^{-1}, which is too large for energy transfer. Therefore, *m*NBA cannot effectively sensitize luminescence emission of Eu^{3+} ion in Complex 1 [55]. Complex 2 has a strong emission intensity with shoulder peaks, which may be ascribed to the crystal field splitting and the asymmetric molecule structure [56].

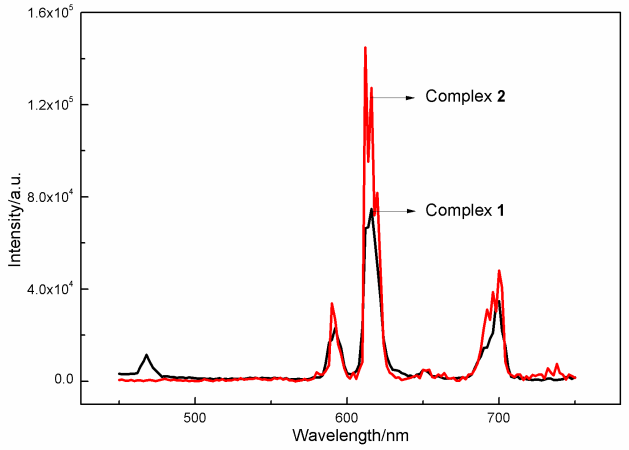

Figure 9. Luminescence spectra of Complexes 1 and 2.

The luminescence lifetimes and quantum efficiencies of the Complexes 1 and 2 are listed in Table 3, and the luminescence decay curves and the corresponding fit curves of $^5D_0$ energy level are shown in Figures 10 and S9, respectively. The relationship between luminescence intensity and lifetime is expressed as $I_{(t)} = I_0 e^{(-t/\tau)}$ that is $Ln(I(t))/I_0 = -k/t = -t/\tau$ (I_0 is the initial luminescence intensity and τ is the luminescence lifetime)[15]. The luminescence lifetimes of Complexes 1 and 2 are 0.761 and 0.447 ms, respectively. The luminescence lifetimes of the complexes are not long, which may result from the fact that the complexes have water molecules, leading to the high nonradiative rates.

In addition, luminescent quantum efficiencies (η) were calculated according to literature [57–60]. The value η mainly depends on lifetime and I_{02}/I_{01}. As can be clearly seen from Table 3, the quantum efficiencies are the reverse of the luminescence intensities of Complexes 1 and 2. Although the radiative transition rates A_r of Complex 1 (328 s^{-1}) are slower than that of complex 2 (374 s^{-1}), the nonradiative A_{nr} of complex 2 (1865 s^{-1}) is much faster than complex 1 (987 s^{-1}). Thus, the quantum efficiency of Complex 1 (25.0%) is higher than that of Complex 2 (16.7%). This shows that the nonradiative energy transfer from the emitting Eu ^{III} ion to the oscillating O-H group of the coordinated water molecules is very easy.

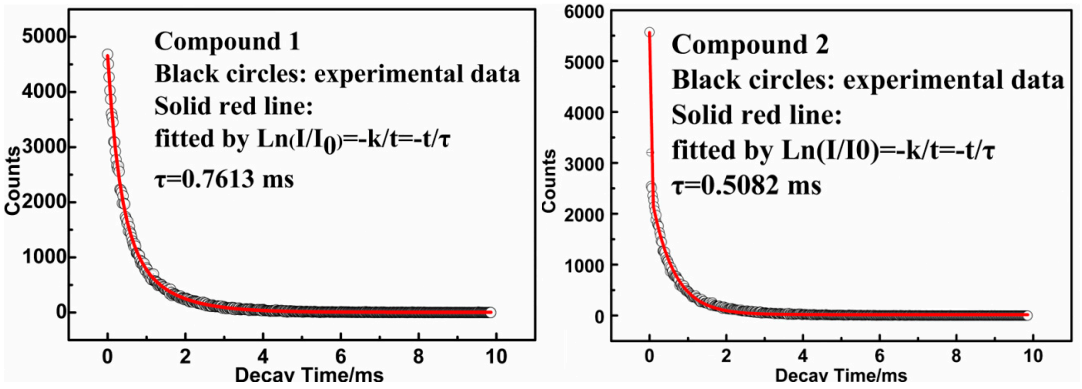

Figure 10. Luminescence decay curves of Complexes 1 and 2.

Table 3. Luminescent quantum efficiency data of Complexes 1 and 2.

Parameters	(1)	(2)
ν_{00} (cm^{-1})	17,271	17,241
ν_{01} (cm^{-1})	16,892	16,949
ν_{02} (cm^{-1})	16,234	16,260
ν_{03} (cm^{-1})	15,385	15,408
ν_{04} (cm^{-1})	14,306	14,368
I_{01} (a.u)	227	339
I_{02} (a.u)	745	1448
I_{02}/ I_{01}	3.28	4.28
τ (ms)	0.761	0.447
$1/\tau$ (ms^{-1})	1.314	2.24
A_r (s^{-1})	328	374
A_{nr} (s^{-1})	987	1865
η (%)	25.0	16.7
χ^2	0.9990	0.9987

4. Conclusions

In summary, five crystals of Eu ^{III}, Yb ^{III} and Er ^{III} with neutral ligands of TPTZ and anion ligands of *m*NBA, H_2BDC and TTA have been synthesized under different synthetic conditions. Among them, Crystal complexes 1 and 3 belong to coordination polymer, and the other three complexes belong to mononuclear crystal. One TPTZ only coordinates with one Ln ^{III} ion. The ligands of organic carboxylic acid tend to adopt multiple coordination modes with Ln ^{III} and form multinuclear complexes. Lanthanide ions have high and variable coordination numbers. When the amount of organic ligands is sufficient in the preparation of the crystal complexes, solvent molecules have difficulty participating in coordination. However, when the organic ligand is lacking, solvent molecules participate in coordination with Ln ^{III} ions. If the amount of ligand is limited and no solvent molecules exist in the reaction system, the coordination number of Ln ^{III} is lower. In addition, TTA is broken down into small molecules at high temperature after long-time reaction. For europium complexes, Complex 2 has a strong emission intensity and relatively low τ and η, which could be ascribed to the composition of the complex and the nonradiative energy transfer from the emitting Eu ^{III} ion to the oscillating O-H group of the coordinated water molecules.

Supplementary Materials: The following are available online at www.mdpi.com/link, Figure S1: Coordination polyhedron of Eu3+ ions in crystal 1; Figure S2: Coordination polyhedron of Eu3+ ions in crystal 2; Figure S3: Coordination polyhedron of Yb3+ ions in crystal 3; Figure S4: The coordination environment of BDC2-and Yb3+ in crystal 3; Figure S5: The 2D layered structure of crystal 3; Figure S6: Coordination polyhedron of Yb3+ ions in crystal 4; Figure S7: Coordination polyhedron of Yb3+ ions in crystal 5; Figure S8: Excitation spectra of complexes 1 and 2; Figure S9: Fluorescence fit curves of complexes 1 and 2. Table S1: Selected Bond lengths [Å] and angles [º]for crystal 1; Table S2: Selected Bond lengths [Å] and angles [º] for crystal 2; Table S3: Selected

Bond lengths [Å] and angles [º] for crystal 3; Table S4: Selected Bond lengths [Å] and angles [º] for crystal 4; Table S5. Selected Bond lengths [Å] and angles [º] for crystal 5.

Acknowledgments: The research work is supported by the National Natural Science Foundation of China (21561023, 51501094, 21161013), the Natural Science Foundation of the Inner Mongolia Autonomous Region of China (2011MS0202), the Opening Foundation for Significant Fundamental Research of the Inner Mongolia Autonomous Region of China (2010KF03), and the Program of High-Level Talents of Inner Mongolia University (21300-5155104).

Author Contributions: Jingjing Li, Haibin Chu, and Yongliang Zhao conceived and designed the experiments. Jingjing Li and Bin Yue performed the experiments. Xueqiong Zhang and Ailing Wang contributed the measurements, analyzed and verified the data. Jingjing Li, Haibin Chu, and Yongliang Zhao wrote the manuscript. Lingjuan Kong and Jian Zhou modified figures. All authors read and approved the final version of the manuscript to be submitted.

Conflicts of Interest: The authors declare that there is no conflict of interest.

References

1. Pointillart, F.; Jung, J.; Berraud-Pache, R.; Le Guennic, B.; Dorcet, V.; Golhen, S.; Cador, O.; Maury, O.; Guyot, Y.; Decurtins, S.; et al. Luminescence and Single-Molecule Magnet Behavior in Lanthanide Complexes Involving a Tetrathiafulvalene-Fused Dipyridophenazine Ligand. *Inorg. Chem*. **2015**, *54*, 5384–5397. doi:10.1021/acs.inorgchem.5b00441.
2. Eliseeva, S.V.; Bünzli, J.C.G. Lanthanide luminescence for functional materials and bio-sciences. *Chem. Soc. Rev*. **2010**, *39*, 189–227. doi:10.1039/B905604C.
3. Hong, Z.R.; Liang, C.J.; Li, R.G.; Zhao, D.; Fan, D.; Li, W.L. Infrared electroluminescence of ytterbium complexes in organic light emitting diodes. *Thin Solid Films* **2001**, *391*, 122–125. doi: 10.1016/S0040-6090(01)00831-8.
4. Stouwdam, J.W.; Hebbink, G.A.; Huskens, J.; van Veggel, F.C.J.M. Lanthanide-Doped Nanoparticles with Excellent Luminescent Properties in Organic Media. *Chem. Mater*. **2003**, *15*, 4604–4616. doi:10.1021/cm034495.
5. Kuriki, K.; Koike, Y.; Okamoto, Y. Plastic Optical Fiber Lasers and Amplifiers Containing Lanthanide Complexes. *Chem. Rev*. **2002**, *102*, 2347–2356. doi:10.1021/cr010309g.
6. Sun, H.J.; Fu, X.T.; Chu, H.B.; Du, Y.; Lin, X.M.; Li, X.; Zhao, Y.L. Synthesis, characterization and luminescence property of ternary rare earth complexes with azatriphenylenes as highly efficient sensitizers.. *J. Photochem. Photobiol. A Chem.* **2011**, *219*, 243–249. doi:10.1016/j.jphotochem.2011.02.026.
7. Wang, R.Y.; Yang, J.; Zheng, Z.P.; Carducci, M.D.; Cayou, T.; Peyghambarian, N.; Jabbour, G.E. First Oxadiazole-Functionalized Terbium(III)*β*-Diketonate for Organic Electroluminescence.. *J. Am. Chem. Soc*. **2001**, *123*, 6179–6180. doi:10.1021/ja004113u.
8. Pettinari, C.; Marchetti, F.; Pettinari, R.; Drozdov, A.; Troyanov, S.; Voloshin, A.L.; Shavaleev, N.M. Synthesis, structure and luminescence properties of new rare earth metal complexes with 1-phenyl-3-methyl-4-acylpyrazol-5-ones.. *J. Dalton Trans*. **2002**, *2*, 1409–1415. doi:10.1039/B108058J.
9. Maghami, M.; Farzaneh, F.; Simpson, J.; Ghiasi, M.; Azarkish, M.J. Synthesis, crystal structure, antibacterial activity and theoretical studies on a novel mononuclear cobalt(II) complex based on 2,4,6-tris(2-pyridyl)-1,3,5-triazine ligand.. *Mol. Struct*. **2015**, *1093*, 24–32. doi:10.1016/j.molstruc.2015.03.037.
10. Therrien, B. Coordination chemistry of 2,4,6-tri(pyridyl)-1,3,5-triazine ligands.. *J. Organomet. Chem.* **2011**, *696*, 637–651. doi:10.1016/j.jorganchem.2010.09.037.
11. Abdi, K.; Hadadzadeh, H.; Salimi, M.; Simpson, J.; Khalaji, A.D. A mononuclear copper(II) complex based on the polypyridyl ligand 2,4,6-tris(2-pyridyl)-1,3,5-triazine (tptz), $[Cu(tptz)_2]^{2+}$: X-ray crystal structure, DNA binding and *in vitro* cell cytotoxicity. *Polyhedron* **2012**, *44*, 101–112. doi:10.1016/j.poly.2012.06.089.
12. Xu, H.W.; Li, J.X.; Pin, L.; Chen, Z.N.; Wu, J.G. Self-assembly luminescent complexes with $[Ag_2(\mu\text{-dppm})_2(MeCN)_2](SbF_6)_2$ and tptz as components. *Transit. Met. Chem.* **2007**, *32*, 839–844. doi:10.1007/s11243-007-0270-y.
13. Tyagi, P.; Singh, U.P. Chloro and azido bonded manganese complexes: synthesis, structural, and magnetic studies. *J. Coord. Chem*. **2009**, *62*, 1613–1622. doi:10.1080/00958970802680682.

14. Zheng, Y.Q.; Xu, W.; Lin, F.; Fang, G.S. Syntheses and crystal structures of copper(II) complexes derived from 2,4,6-tris(2-pyridyl)-1,3,5-triazine. *J. Coord. Chem*. **2006**, *59*, 1825–1834. doi:10.1080/00958970600571760.
15. Klink, S.I.; Grave, L.; Reinhoudt, D.N.; van Veggel, F.C.J.M.; Werts, M.H.V.; Geurts, F.A.J.; Hofstraat, J.W. A Systematic Study of the Photophysical Processes in Polydentate Triphenylene-Functionalized Eu^{3+}, Tb^{3+}, Nd^{3+}, Yb^{3+}, and Er^{3+} Complexes. *J. Phys.Chem.* **2000**, *104*, 5457–5468. doi:10.1021/jp994286.
16. Silva, C.R.D.; Wang, J.F.; Carducci, M.D.; Rajapakshe, S.A.; Zheng, Z.P. Synthesis, structural characterization and luminescence studies of a novel europium(III) complex $[Eu(DBM)_3(TPTZ)]$ (DBM: dibenzoylmethanate; TPTZ: 2,4,6-tri(2-pyridyl)-1,3,5-triazine). *Inorg. Chim. Acta* **2004**, *357*, 630–634. doi:10.1016/j.ica.2003.08.006.
17. Yue, B.; Chen, Y.N.; Chu, H.B.; Qu, Y.R.; Wang, A.L.; Zhao, Y.L. Synthesis, crystal structures and fluorescence properties of dinuclear Tb(III) and Sm(III) complexes with 2,4,6-tri(2-pyridyl)-1,3,5-triazine and halogenated benzoic acid.. *Inorg. Chim. Acta.* **2014**, *414*, 39–45. doi:10.1016/j.ica.2014.01.024.
18. Nawrot, I.; Machura, B.; Kruszynski, R. Thiocyanate cadmium(II) complexes of 2,4,6-tri(2-pyridyl)-1,3,5-triazine – Synthesis, structure and luminescence properties.. *J. Lumin*. **2014**, *156*, 240–254. doi:10.1016/j.jlumin.2014.08.022.
19. Liao, J.H.; Hwang, W.S.; Chen, G.Y. Synthesis, Characterization, and Photoluminescence of Lanthanide-containing Coordination Polymers Constructed from 4,4′-Biphenyldicarboxylate and 2,4,6-Tris(2-pyridyl)-1,3,5-triazine Ligands.. *Z. Anorg. Allg. Chem*. **2014**, *640*, 1793–1798. doi:10.1002/zaac.201300619.
20. Abdi, K.; Hadadzadeh, H.; Weil, M.; Rudbari, H.A. Mono- and polynuclear copper(II) complexes based on 2,4,6-tris(2-pyridyl)-1,3,5-triazine and its hydrolyzed form.. *Inorg. Chim. Acta*. **2014**, *416*, 109–121. doi:10.1016/j.ica.2014.03.021.
21. Zhang, F.; Bei, F.L.; Cao, J.M. Sovolthermal Synthesis and Crystal Structure of Two CdII Coordination Polymers of Benzenedicarboxylic. *J.Chem. Crystallogr*. **2008**, *38*, 561–565. doi: 10.1007/s10870-008-9336-8.
22. Huang, F.P.; Tian, J.L.; Chen, G.J.; Li, D.D.; Gu, W.; Liu, X.; Yan, S.P.; Liao, D.Z.; Cheng, P. A case study of the ZnII-BDC/bpt mixed-ligand system: positional isomeric effect, structural diversification and luminescent properties. *CrystEngComm*. **2010**, *12*, 1269–1279. doi:1039/B915506F.
23. Daiguebonne, C.; Kerbellec, N.; Bernot, K.; Gérault, Y.; Deluzet, A.; Guillou, O. Crystal Structure, and Porosity Estimation of Hydrated Erbium Terephthalate Coordination Polymers.. *Inorg. Chem*. **2006**, *45*, 5399–5406. doi:10.1021/ic060241t.
24. Guo, X.D.; Zhu, G.S.; Sun, F.X.; Li, Z.Y.; Zhao, X.J.; Li, X.T.; Wang, H.C.; Qiu, S.L. Synthesis, Structure, and Luminescent Properties of Microporous Lanthanide Metal−Organic Frameworks with Inorganic Rod-Shaped Building Units. *Inorg. Chem*. **2006**, *45*, 2581–2587. doi: 10.1021/ic0518881.
25. Biswas, S.; Ahnfeldt, T.; Stock, N. New Functionalized Flexible Al-MIL-53-X (X = -Cl, -Br, -CH3, $-NO_2$, $-(OH)_2$) Solids: Syntheses, Characterization, Sorption, and Breathing Behavior. *Inorg. Chem*. **2011**, *50*, 9518–9526. doi**:**10.1021/ic201219g.
26. Loiseau, T.; Serre, C.; Huguenard, C.; Fink, G.; Taulelle, F.; Henry, M.; Bataille, T.; Férey, G. A Rationale for the Large Breathing of the Porous Aluminum Terephthalate (MIL-53) Upon Hydration. *Chemistry* **2004**, *10*, 1373–1382. doi: 10.1002/chem.200305413.
27. Lu, Y.; Yan, B. A novel luminescent monolayer thin film based on postsynthetic method and functional linker. *J. Mater. Chem*. **2014**, *2*, 5526–5532. doi: 10.1039/C4TC00578C.
28. Ni, Y.; Tao, J.; Lu, C.H.; Xu, Z.Z.; Kang, Z.T.; Xu, F.J. Synthesis and luminescence properties of ternary complexes of $Sm_xTb_{b-x}(TTA)_3Phen$ nanoparticles and their surface modification.. *Mater. Sci*. **2013**, *48*, 5309–5315. doi: 10.1007/s10853-013-7325-6.
29. Yu, X.K.; Lin, C.J.; Zheng, Y.Q.; Zhu, H.L. Crystal structures, magnetic, dielectric and ferroelectric properties of two copper(II) complexes with m-nitrobenzoic acid. *Transit. Met. Chem*. **2014**, *39*, 71–79. doi: 10.1007/s11243-013-9776-7.
30. Binnemans, K. Lanthanide-Based Luminescent Hybrid Materials. *Chem. Rev*. **2009**, *109*, 4283–4374. doi: 10.1021/cr8003983.
31. Liao, S.; Yang, X.; Jones, R.A. Self-Assembly of Luminescent Hexanuclear Lanthanide Salen Complexes. *Cryst.Growth Des*. **2012**, *12*, 970–974. doi: 10.1021/cg201444p.

32. Pan, L.; Gao, X.H.; Lv, X.C.; Tan, Z.C.; Gao, H. Crystal structure and properties of complexes [Ln(Gly)4Im·(ClO4)4]n (Ln:Nd, Sm) constructed from eight-coordination containing square antiprism. *J. Mol. Struct*. **2016**, *1117*, 57–63. doi: 10.1016/j.molstruc.2016.03.049.
33. Zhong, J.X.; Zhang, H.H.; Gao, X.; Qu, Y.C.; Wu, J.Z.; Cai, Y.P. Crystal structures and luminescent properties modulated by auxiliary ligands for series of lanthanide coordination polymers with triazole-benzoic acid. *Inorg. Chem. Commun*. **2016**, *71*, 1–4. doi: 10.1016/j.inoche.2016.06.024.
34. Wang, Y.; Jin, C.W.; He, S.M.; Ren, N.; Zhang, J.J. Five novel lanthanide complexes with 2-chloroquinoline-4-carboxylic acid and 1,10-phenanthroline: Crystal structures, molecular spectra, thermal properties and bacteriostatic activities. *J. Mol. Struct*. **2016**, *1125* 383–390. doi:10.1016/j.molstruc.2016.07.007.
35. Al-Assy, W.H.; El-Askalany, A.M.H.; Mostafa, M.M. Structural comparative studies on new MnII, CrIII and RuIII complexes derived from 2,4,6-tri-(2-pyridyl)-1,3,5-triazine (TPTZ). *Spectrochim. Acta Part A* **2013**, *116*, 401–407. doi:10.1016/j.saa.2013.07.086.
36. Teoh, S.G.; Ang, S.H.; Declercq, J.P. Synthesis and characterization of di-*n*-butylbis(2,4-dihydroxybenzoato tin(IV). *J. Polyhedron* **1997**, *16*, 3729–3733. doi:10.1016/S0277-5387(97)00152-6.
37. Deacon, G.B.; Phillips, R.J. Relationships between the carbon-oxygen stretching frequencies of carboxylato complexes and the type of carboxylate coordination. *Coord. Chem. Rev*. **1980**, *33*, 227–250. doi:10.1016/S0010-8545(00)80455-5.
38. Qu, Y.R.; Lin, X.M.; Wang, A.L.; Wang, Z.X.; Kang, J.; Chun, H.B.; Zhao, Y.L. Study on silicon oxide coated on silver nanocrystal to enhance fluorescence intensity of rare earth complexes. *J. Lumin*. **2014**, *154*, 402–409. doi:10.1016/j.jlumin. 2014.05.013.
39. Wang, A.L.; Zhou, D.; Chen, Y.N.; Li, J.J.; Zhang, H.X.; Zhao, Y.L.; Chu, H.B. Crystal structure and photoluminescence of europium, terbium and samarium compounds with halogen-benzoate and 2,4,6-tri(2-pyridyl)-s-triazine. *J. Lumin*. **2016**, *177*, 22–30. doi:10.1016/j.jlumin. 2016.04.024.
40. Chen, N.; Ji, L.; Du, G.P. Luminescent properties of hybrid nanostructures of ion-exchanged Y_2O_3:Eu^{3+}nanoparticles with 2-thenoyltrifluoroacetone ligands. *J. Lumin*. **2014**, *153*, 259–263. doi:10.1016/j.jlumin.2014.03.042.
41. Xu, C.J.; Wan, J.T.; Li, B.G. Monochromatic light-emitting copolymer of methyl methacrylate and Eu-complexed 5-acrylamido-1,10-phenanthroline. *Dyes Pigment.* **2013**, *98*, 493–498. doi:10.1016/j.dyepig.2013.04.001.
42. Liu, Q.Q.; Geng, J.; Wang, X.X.; Gu, K.H.; Huang, W.; Zheng, Y.X. Luminescent lanthanide(III)-cored complexes based on the combination of 2-(5-bromothiophen)imidazo[4,5-f][1,10]phenanthroline and 2-thenoyltrifluoroacetonate ligands. *Polyhedron* **2013**, *59*, 52–57. doi:10.1016/j.poly.2013.04.036.
43. Ni, Y.R.; Tao, J.; Jin, J.Y.; Lu, C.H.; Xu, Z.Z.; Xu, F.; Chen, J.M.; Kang, Z.T. An investigation of the effect of ligands on thermal stability of luminescent samarium complexes.. *J. Alloy. Compd*. **2014**, *612*, 349–354. doi:10.1016/j.jallcom.2014.05.211.
44. Zhao, L.F.; Chen, Y.S.; Bao, L. Synthesis and crystal structure of rare earth complexes with o-nitrobenzoic acid and N,N-dimethylformamide.. *J. Mol. Struct*. **2010**, *966*, 48−52. doi:10.1016/j.molstruc.2009.12.003.
45. Zhao, H.H.; Lopez, N.; Prosvirin, A.; Chifotides, T.H.; Dunbar, K.R. Lanthanide–3d cyanometalate chains Ln(III)–M(III) (Ln =Pr,Nd,Sm,Eu,Gd,Tb;M= Fe) with the tridentate ligand 2,4,6-tri(2-pyridyl)-1,3,5-triazine(tptz): evidence of ferromagnetic interactions for the Sm(III)–M(III) compounds (M = Fe, Cr). *Dalton Trans*. **2007**, *8*, 878–888. doi:10.1039/B616016F.
46. Song, T.Y.; Chen, P.; Xu, J.N.; Zhang, L.R. *Inorganic Chemistry*; Higher Education Press: Beijing, China, 2015.
47. Al-Assy, W.H.; Mostafa, M.M. Comparative studies and modeling structures of two new isomers containing binuclear PdII complexes derived from 2,4,6-tri-(2-pyridyl)-1,3,5-triazine (TPTZ). *Spectrochim. Acta Part A* **2014**, *120*, 568–573. doi:10.1016/j.saa.2013.10.118.
48. Luo, J.; Qiu, L.J.; Liu, B.Z.; Zhang, X.R.; Yang, F.; Cui, L.L. Synthesis, Structure and Magnetic Properties of Two Cobalt(II) Dicyanamide (dca) Complexes with Heterocyclic Nitrogen Donors Tetra(2-pyridyl)pyrazine (tppz) and 2,4,6-Tri(2-pyridyl)-1,3,5-triazine (tptz): [Co_2(tppz)(dca)$_4$]CH_3CN and [Co(tptz)(dca)(H_2O)](dca).. *Chin. J. Chem*. **2012**, *30*, 522–528. dol: 10.1002/cjoc.201100553.
49. Handa, M.; Scheidt, K.A.; Bossart, M.; Zheng, N.; Roush, W.R. Two new silver(I) complexes with 2,4,6-tris(2-pyridyl)-1,3,5-triazine (tptz): Preparation, characterization, crystal structure and alcohol oxidation activity in the presence of oxone.. *Polyhedron* **2010**, *29*, 2837–2843. dol:10.1016/j.poly.2010.07.005.

50. Liu, C.M.; Xiong, M.; Zhang, D.Q.; Du, M.; Zhu, D.B. Two- and three-dimensional lanthanide–organic frameworks constructed using 1-hydro-6-oxopyridine-3-carboxylate and oxalate ligands. *Dalton Trans*. **2009**, *29*, 5666–5672. doi**:**10.1039/B903613J**.**
51. Ofelt, G.S. Intensities of Crystal Spectra of Rare-Earth Ions. *J. Chem. Phys*. **1962**, *37*, 511–520. doi:10.1063/1.1701366.
52. Sivakumar, S.; Reddy, M.L.P.; Cowley, A.H.; Vasudevan, K.V. Synthesis and crystal structures of lanthanide 4-benzyloxy benzoates: Influence of electron-withdrawing and electron-donating groups on luminescent properties. *Dalton Trans*. **2010**, *39*, 776–786. doi:10.1039/B917256D.
53. Biju, S.; Reddy, M.L.P.; Cowley, A.H.; Vasudevan, K.V. 3-Phenyl-4-acyl-5-isoxazolonate complex of Tb3+ doped into poly-β-hydroxybutyrate matrix as a promising light-conversion molecular device. *J. Mater. Chem*. **2009**, *19*, 5179–5187. doi:10.1039/B905304B.
54. Ramya, A.R.; Reddy, M.L.P.; Cowley, A.H.; Vasudevan, K.V. Synthesis, Crystal Structure, and Photoluminescence of Homodinuclear Lanthanide 4-(Dibenzylamino)benzoate Complexes. *Inorg. Chem*. **2010**, *49*, 2407–2415. doi**:** 10.1021/ic902257u.
55. Bettencourt-Dias, A.D.; Viswanathan, S. Nitro-functionalization and luminescence quantum yield of Eu(III) and Tb(III) benzoic acid complexes. *Dalton Trans*. **2006**, *250*, 4093–4103. doi: 10.1039/B606970C.
56. Kang, J.G.; Na, M.K.; Yoon, S.K.; Sohn, Y.; Kim, Y.D.; Suh, I.H. Determination of the structure of EuTETA and the luminescence properties of EuTETA and EuDOTA (TETA=1,4,8,11-tetraazacyclotetradecane-1,4,8,11-tetraacetate and DOTA=1,4,7,10-tetraazacyclododecane-1,4,7,10-tetraacetate). *Inorg. Chim. Acta* **2000**, *310*, 56–64. doi:10.1016/S0020-1693(00)00268-1.
57. Wang, A.L.; Zhou, D.; Wei, X.Y.; Wang, Z.X.; Qu, Y.R.; Zhang, H.X.; Chen, Y.N.; Li, J.J.; Chu, H.B.; Zhao, Y.L. Luminescence properties and crystal structure of europium complexes with phenoxyacetic acid and 2,4,6-tri(2-pyridyl)-s-triazine. *J. Lumin*. **2015**, *160*, 238–244. doi:10.1016/j.jlumin.2014.12.013.
58. Frey, S.T.; Gong, M.L.; Horrocks, W.D., Jr. synergistic Coordination in Ternary Complexes of Eu3+ with Aromatic .beta.-Diketone Ligands and 1,10-Phenanthroline.. *Inorg. Chem*. **1994**, *33*, 3229–3234. doi:10.1021/ic00093a006.
59. Malta, O.L.; Batista, H.J.; Carlos, L.D. Overlap polarizability of a chemical bond: a scale of covalency and application to lanthanide compounds. *Chem. Phys*. **2002**, *282*, 21–30. doi:10.1016/S0301-0104(02)00631-6.
60. Binnemans, K.; Lenaerts, P.; Driesen, K.; Walrand, C.A.G. A luminescent tris(2-thenoyltrifluoroacetonato)europium(III) complex covalently linked to a 1,10-phenanthroline-functionalised sol–gel glass.. *J. Mater. Chem*. **2004**, *14*, 191–195. doi: 10.1039/B311128H.